Short Paper

Bias-Dependent Microwave Characteristics of Atomic Planar-Doped AlGaAs/InGaAs/GaAs Double Heterojunction MODFET's

Y K. CHEN, G W. WANG, D. C. RADULESCU, A. N. LEPORE, P. J. TASKER, L. F. EASTMAN, FELLOW, IEEE, AND ERIC STRID, MEMBER, IEEE

Abstract—**Double heterojunction AlGaAs/InGaAs/GaAs modulation-doped field effect transistors (MODFET's) using lattice-strained AlGaAs/InGaAs/GaAs layer structure have been fabricated and evaluated at microwave frequencies for various bias conditions. MODFET's with a 1-μm gate length show a room-temperature peak extrinsic dc transconductance (g_m) of 400 mS/mm with a full channel current of 610 mA/mm. For 0.3-μm-gate MODFET's an extrinsic dc g_m of 505 mS/mm and a full channel current of 720 mA/mm were obtained. Devices having a 1-μm gate length show a maximum available gain cutoff frequency (f_{max}) of 85 GHz and a current-gain cutoff frequency (f_T) of 22 GHz from S-parameter measurements. The 0.3-μm devices show an f_T of 45 GHz and an f_{max} of 120 GHz. Bias-dependent equivalent circuit models are also discussed.**

I. Introduction

Modulation-doped field-effect transistors (MODFET's) have demonstrated excellent microwave performance with very high cutoff frequency and very good low-noise performance [1]. However, the current-driving capability of conventional single-heterojunction MODFET's is limited by their sheet charge density of less than $1.0\times10^{12}\text{cm}^{-2}$; therefore their power performance and switching speed, which are directly related to current-driving capability, were not much better than the MESFET's. Multiple heterojunction devices [2–4] were then investigated to increase the current density. So far, the highest maximum channel current reported is 600 mA/mm from sixfold GaAs/AlGaAs heterojunctions [2] and 430 mA/mm from lattice-strained AlGaAs/InGaAs/GaAs double heterojunction [4]. Since all these multiple heterojunction devices rely on uniformly doped AlGaAs layers to supply the two-dimensional electron gas (2DEG), the AlGaAs layer has to be highly doped to achieve high 2DEG sheet charge density. This highly doped AlGaAs layer leads to problems such as low breakdown voltage, low activation efficiency of dopants, and poor pinch-off characteristics.

We have reported double heterojunction MODFET structures [5] which utilize two silicon atomic planar-doped AlGaAs layers. This doping technique offers good charge control of the 2DEG density as well as good breakdown behavior. Very little light sensitivity was observed at low temperature (77 K) because of the much reduced region of the heavily doped AlGaAs layer. In this paper, we report the fabrication and characterization of lattice-strained AlGaAs/InGaAs/GaAs double heterojunction MODFET's under various bias conditions for microwave applications.

Manscript received June 11, 1987; revised August 17, 1987. This work was supported in part by the General Electric Company (Syracuse, NY), the Joint Service Electronics Program, ONR, and ARO.

This paper was inadvertently omitted from the *MTT-S International Microwave Symposium Digest*.

Y K Chen, G W. Wang, D. C. Radulescu, A. N. Lepore, P J. Tasker, and L. F Eastman are with the School of Electrical Engineering and the National Nanofabrication Facility, Cornell University, Ithaca, NY 14850

E Strid is with Cascade Microtech Inc., Beaverton, OR.

IEEE Log Number 8717682.

II. Device Structure and Fabrication

The structure is grown by MBE on top of a semi-insulating GaAs substrate in the following sequence: 5000 Å of superlattice buffer layer, 50 Å undoped AlGaAs, Si doping plane with a density of 2×10^{12} cm^{-2}, 85 Å undoped AlGaAs, 200 Å undoped InGaAs channel, 30 Å undoped AlGaAs spacer layer, Si doping plane with a density of 6×10^{12} cm^{-2}, 250 Å undoped AlGaAs, and 400 Å GaAs cap layer doped to 1×10^{18} cm^{-3}. The mole fractions of aluminum and indium are 30 percent and 15 percent, respectively.

The grown wafers were fabricated with a recess gate FET process. After device isolation by mesa etch, source and drain ohmic contacts were defined by optical lithography. Ni/AuGe/Pd/Au were subsequently evaporated and lifted off. Rapid thermal annealer was used to alloy the metals at 450°C for 10 seconds to form the ohmic contacts. A typical specific contact resistivity of 0.1 $\Omega\cdot$mm was obtained from the transmission line measurement. A mid-UV contact aligner is used to define the 1-μm gate, while the electron beam lithography is used to write the 0.3-μm gate pattern. Channel current was adjusted by recess etch before evaporation of Ti/Pd/Au to form the gate electrodes.

III. DC Characteristics

Fig. 1 shows the room-temperature $I-V$ characteristics of a fabricated 1×100 μm MODFET. The peak extrinsic dc g_m is 400 mS/mm with a maximum channel current of 610 mA/mm. The $I-V$ characteristics of a 0.3×100 μm MODFET are shown in Fig. 2. A peak extrinsic g_m of 505 mS/mm is obtained. This 0.3-μm device shows very good output conductance and pinch-off characteristics because of the improved carrier confinement in the quantum well [6]. Fig. 3 shows the conduction band diagram of the planar-doped quantum well structure. The threshold voltage (V_T) of the double heterojunction MODFET can be derived by solving a one-dimensional Poisson's equation with the help of the band diagram:

$$V_T = \Phi_B - \left[qN_{d1}d_1/\epsilon_1 + \left(\epsilon_3/\epsilon_1(d_1+W_1) + \epsilon_3 L/\epsilon_2 + W_2\right) qN_{d2}/\epsilon_3 \right] - \left(\delta + \Delta E_{c1} - \Delta E_{c2} + E_0\right)/q \quad (1)$$

where Φ_B is the Schottky barrier height and E_0 is the ground-state energy of 2DEG. N_{d1} and N_{d2} are the silicon sheet doping densities in the AlGaAs and GaAs layers; w_1 and w_2 are the corresponding spacer layer thickness; and d_1 and L are the thickness for the undoped AlGaAs layer and the quantum well. ΔE_{c1} and ΔE_{c2} are the discontinuities of the conduction bands; δ is the difference of the doped GaAs conduction band minimum and the Fermi energy; and ϵ_1, ϵ_2, and ϵ_3 are the permittivities of AlGaAs, InGaAs, and GaAs, respectively. From this equation, V_T is a linear function of d_1 in this planar-doped MODFET

0018-9480/87/1200-1456$01.00 ©1987 IEEE

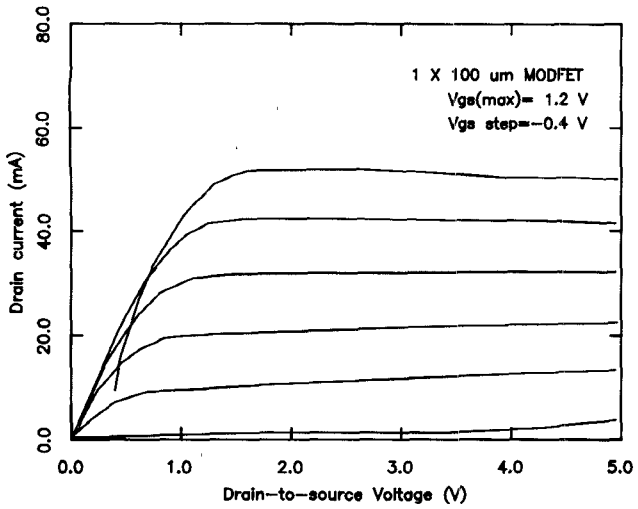

Fig. 1 $I-V$ characteristics of 1×100 μm MODFET.

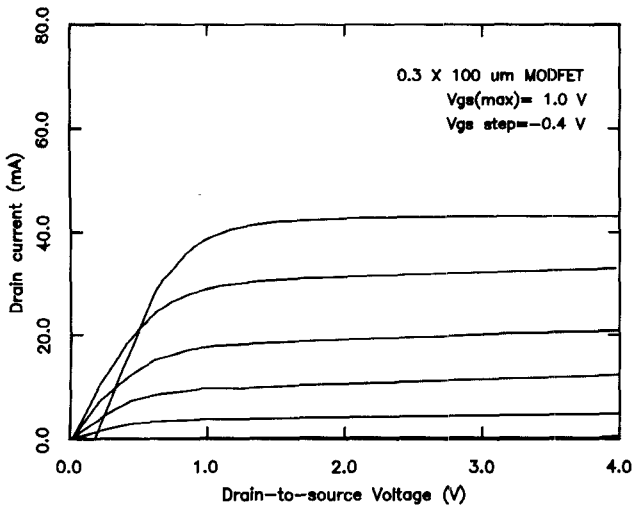

Fig. 2. $I-V$ characteristics of 0.3×100 μm MODFET.

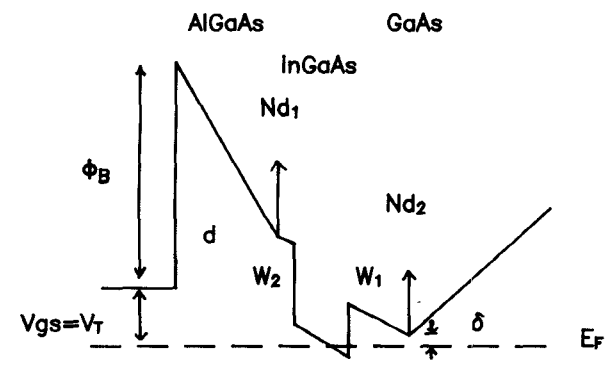

Fig. 3 Conduction band diagram of the planar-doped quantum-well MODFET structure.

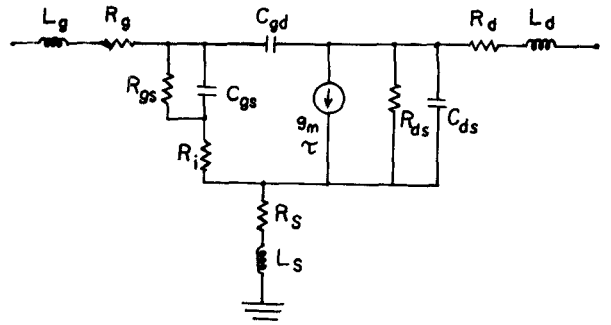

Fig. 4. MODFET equivalent circuit model.

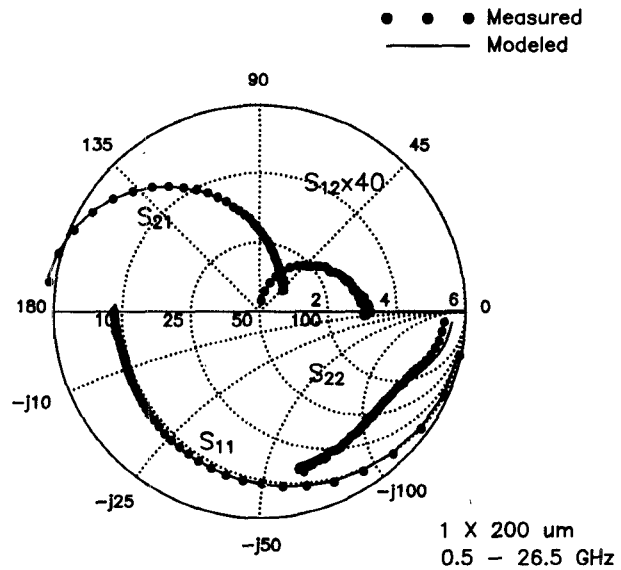

Fig. 5 Measured and modeled S-parameters of a 1-μm MODFET.

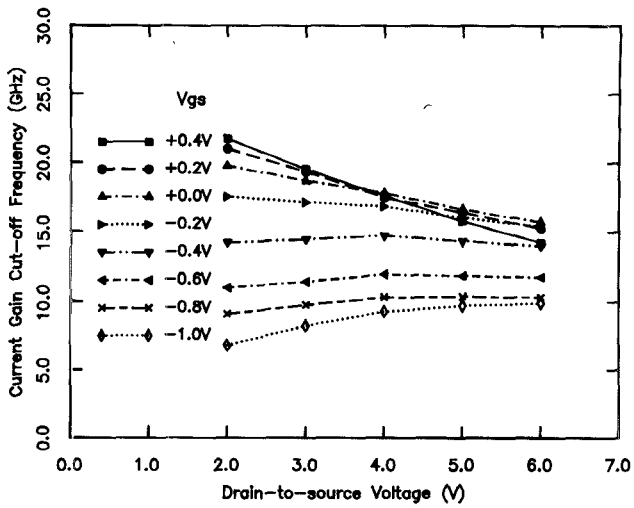

Fig. 6. Current gain cutoff frequency (f_T) at various bias points.

structure in comparison with the conventional square rule dependence of the uniformly doped structures.

IV. Microwave Performance

Microwave measurements have been performed from 0.5 to 26.5 GHz in 0.5-GHz steps with a pair of Cascade Microtech's microwave wafer probes and an HP8510 automatic network analyzer. S-parameter data have been taken with the gate and drain biased at various voltages, and fitted to the equivalent circuit model depicted in Fig. 4 through the computer optimization program FETFITTER. Good agreement between the measured and modeled S parameters of a 1×200 μm MODFET is shown in Fig. 5. Figs. 6 and 7 show the bias-dependent f_T's and f_{max}'s of the 1×200 μm MODFET, calculated by using [7]

$$f_T=\frac{g_m}{2\pi C_{gs}} \tag{2}$$

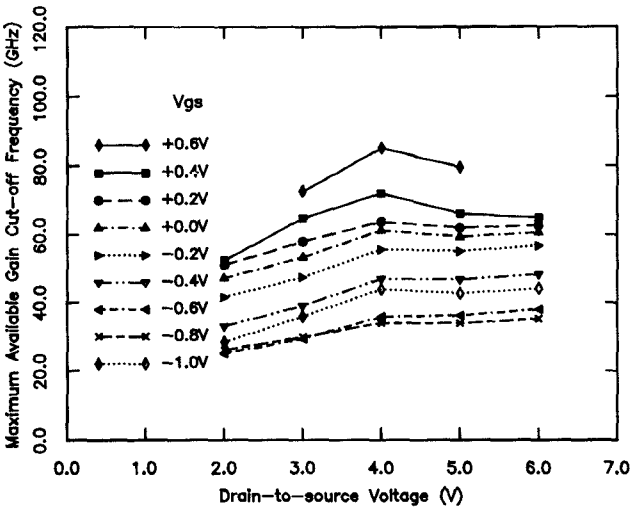

Fig 7 Maximum available gain cutoff frequency (f_{max}) at various bias points.

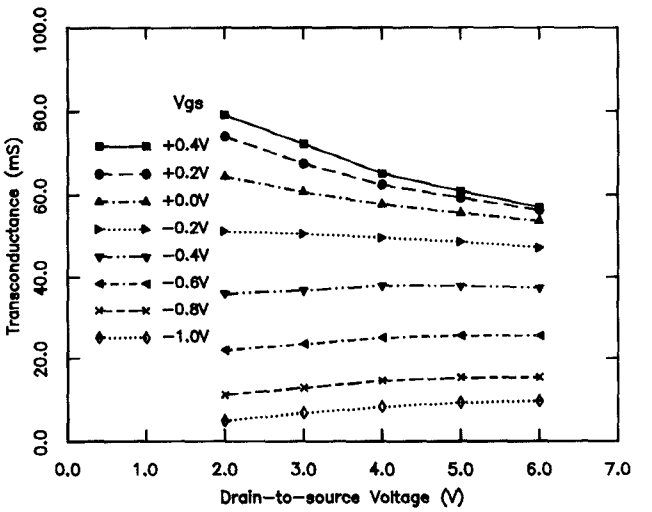

Fig. 9. Transconductance (g_m) versus gate and drain bias.

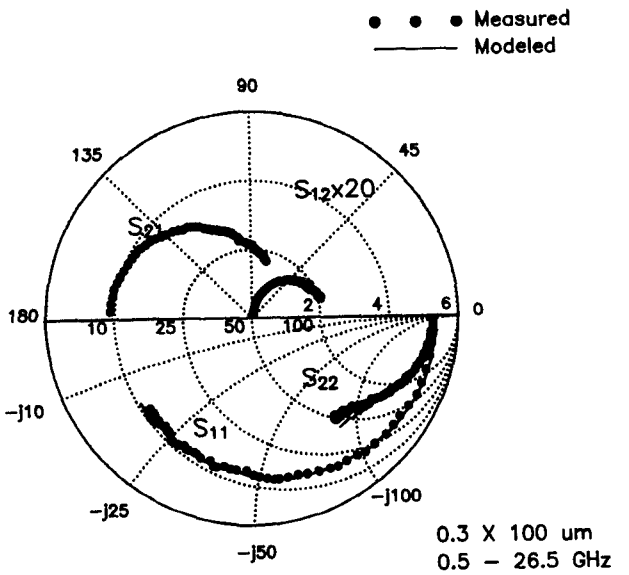

Fig 8 Measured and modeled S-parameters of a 0.3-μm MODFET.

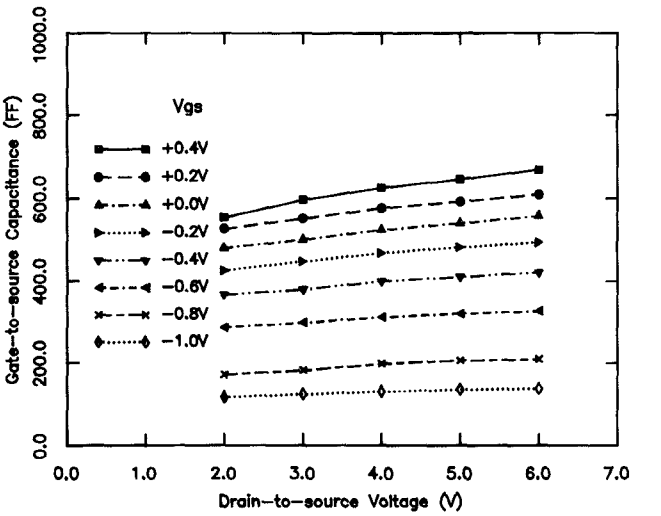

Fig. 10. Gate-to-source capacitance (C_{gs}) versus gate and drain bias.

and

$$f_{max} = \frac{f_T}{\left[4(R_{in}+R_s+R_G)/R_{ds}+4\pi f_T C_{dq}(R_{in}+R_s+R_G)\right]^{1/2}} \quad (3)$$

because the stability factor (k) may not be greater than unity over the whole measured frequency for certain bias points. The 1-μm device is biased at $V_{gs} = 0.6$ V and $V_{ds} = 2$ V for a maximum f_T of 22 GHz. The maximum f_{max} of 85 GHz is obtained at $V_{gs} = 0.6$ V and $V_{ds} = 4$ V. This is the highest reported f_{max} of either GaAs MESFET's or MODFET's with 1-μm gate length. The drain voltage for the maximum f_{max} is higher than that for the maximum f_T because of higher R_{ds} and lower C_{gd} from the wider AlGaAs depletion region between gate and drain. The measured and modeled S-parameters of the 0.3×100 μm device are shown in Fig. 8, with an f_T of 45 GHz and an f_{max} of 120 GHz. The excellent dc and microwave performances are the result of good charge control and good carrier confinement through the planar-doped quantum well structure.

V. Bias-Dependent Equivalent Circuit Model

In order to investigate the nonlinear behavior of the double heterojunction MODFET for large-signal applications, the elements of the equivalent circuit have to be examined closely for their bias dependence [8]. The measured S-parameters of the 1×200 μm MODFET at various gate and drain biases are used to determine the bias-dependent equivalent circuit parameters. All these S-parameter measurements are performed while the MODFET is biased in the current saturation region. The external device parasitics such as L_g, R_g, L_d, R_d, L_s, and R_s are assumed to be linear and invariant to the biases. The bias dependence of other elements, including g_m, C_{gs}, C_{gd}, τ, C_{ds}, R_{ds}, and R_{in}, are depicted in Figs. 9–14.

Because of the high aspect ratio (ratio of the gate length to the thickness of active layer) of MODFET's [9], the bias dependence of g_m in Fig. 9 shows less sensitivity to the V_{ds} variation. However, g_m decreases as V_{ds} increases at positive gate bias. This deterioration of g_m is caused by the real-space transfer of hot electrons from the quantum well into the AlGaAs layer and their subsequent removal through the forward-biased gate [10], [11].

For a given drain voltage, C_{gs} increases monotonically with increasing V_{gs}, as shown in Fig. 10. The influence of V_{gs} on C_{gs}

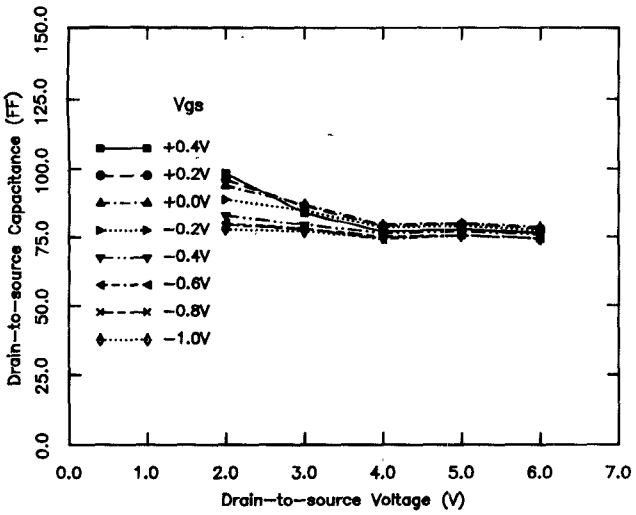

Fig. 11. Drain-to-source capacitance (C_{ds}) versus gate and drain bias.

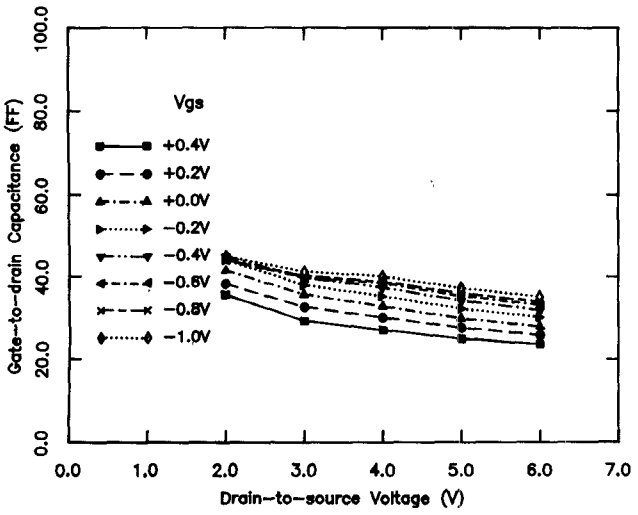

Fig. 12. Gate-to-drain capacitance (C_{gd}) versus gate and drain bias.

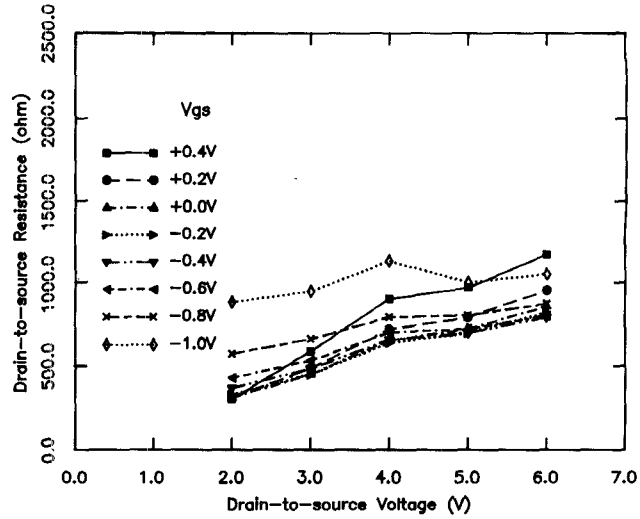

Fig. 13 Output resistance (R_{ds}) versus gate and drain bias.

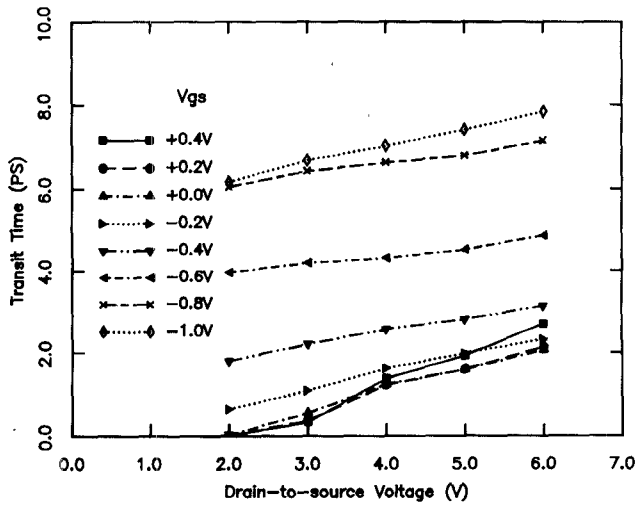

Fig. 14. Transit time (τ) versus gate and drain bias.

cannot be fully explained by the basic charge-control theory of 2DEG [12]. The stronger dependence of C_{gs} on V_{gs} is possibly due to additional charge modulation in the AlGaAs layer [13]. When the gate is biased above 0.2 V, the parallel conduction in the AlGaAs layer starts and V_{gs} only modulates the charges in AlGaAs layer [14]. The slight increase of C_{gs} with increasing V_{ds} is therefore due to the increase of the depletion region between gate and drain as in the case of GaAs MESFET [8].

C_{ds} is dominated by the parasitic capacitance from drain to source through the active layers and the substrate, and is much less sensitive to the changes of the gate and drain biases (Fig. 11). Similar bias dependence of C_{ds} was also found in the MESFET structures [8]. The capacitive coupling (C_{gd}) between gate and drain is through the gate fringing field. C_{gd} is reduced as the gate depletion region penetrates toward the drain with increasing potential difference, as shown in Fig. 12.

The values of R_{ds} shown in Fig. 13 are very high due to the excellent carrier confinement through the quantum well structure. This kind of confinement is very essential for the high-frequency performance of devices with short gate length. The increase of R_{ds} with increasing V_{ds} is caused by extended depletion region between gate and drain. Nevertheless, the increasing gate current due to real-space-transfer hot electrons comes into play when V_{gs} is above 0.2 V, and R_{ds} shows abnormal behavior.

The carrier transit time effect under the gate is denoted by τ. As effective gate length is determined by the depletion region, the bias dependence of τ in Fig. 14 is due to the variation of depletion region controlled by $|V_{ds} - V_{gs}|$.

VI. Conclusions

We have fabricated and characterized AlGaAs/InGaAs/GaAs double heterojunction MODFET's with 1-μm and 0.3-μm gate lengths. Excellent microwave performance has been achieved, with an f_T of 22 GHz and an f_{max} of 85 GHz from the 1-μm device, and an f_T of 45 GHz and an f_{max} of 120 GHz from the 0.3-μm device.

Bias-dependent equivalent circuit models have been determined to study the nonlinear behavior of the 1-μm device under large-signal conditions. In general, the bias-dependent circuit parameters of MODFET's behave in a way quite similar to those of GaAs MESFET's. Distinctive features of MODFET's, such as heterojunction charge control, AlGaAs parallel conduction, quantum well carrier confinement, and real-space transfer, make the bias dependence of circuit parameters more complicated. This study will be helpful in understanding the device

physics and in optimizing MODFET structures. It also provides valuable information for constructing the large-signal model for computer-aided design and simulation of nonlinear microwave and high-speed digital MODFET integrated circuits.

Acknowledgment

The authors appreciate the courtesy of Spectrum Technology Inc. for providing GaAs substrates for this study.

References

[1] P. C. Chao, P M Smith, U. K. Mishra, S C Palmeteer, K. H. Duh, and J C. M. Hwang, "Quarter-micron low-noise high electron mobility transistors," in *Proc IEEE/Cornell Conf. Adv. Concepts in High-Speed Semicond Dev. and Circuits*, July 1985, pp. 163–171.

[2] P. Saumier and J W Lee, "High-efficiency millimeter-wave GaAs/GaAlAs power HEMT's," *IEEE Electron Device Lett.*, vol EDL-7, pp 503–505, Sept 1986

[3] A K Gupta, R T. Chen, E. A Sovero, and J. A Higgins, "Power saturation characteristics of GaAs/AlGaAs HEMTs," in *Proc. IEEE 1985 MMIC Symp.*, June 1985, pp. 50–53

[4] T Henderson, J. Klem, C K. Peng, J. S Gedymin, W. Kopp, and H. Morkoc, "DC and microwave characteristics of a high current double interface GaAs/InGaAs pseudomorphic MODFET," *Appl. Phys. Lett*, vol no 16, pp 1080–1082, Apr 1986

[5] Y K Chen, D C. Radulescu, P. J. Tasker, G. W. Wang, and L. F. Eastman, "DC and RF characterization of an atomic planar doped double heterojunction MODFET," presented at 1986 Int. GaAs and Related Compound Symp., Las Vegas, NV, Sept. 1986

[6] Y K Chen, D C Radulescu, G. W. Wang, P. J. Tasker, and L F. Eastman, Enhancement of 2DEG density in GaAs/InGaAs/AlGaAs double heterojunction power MODFET structures by buried superlattice and buried p^+ – GaAs buffer layers," *Tech. Dig* 1987 *45th Ann Dev Res Conf*, (Santa Babara CA), June 1987.

[7] P Wolf, "Microwave properties of Schottky-barrier field effect transistor," *IBM J. Res Develop.*, vol. 14, pp. 125–141, Mar. 1970

[8] H A. Willing, C. Rauscher, and P de Santis, "A technique for predicting large-signal performance of a GaAs MESFET," *IEEE Trans Microwave Theory Tech*, vol. MTT-26, pp. 1017–1023, Dec. 1978

[9] M B. Das, "A high aspect ratio design approach to millimeter-wave HEMT structures," *IEEE Trans Electron Devices*, vol ED-32, pp. 11–17, Jan 1985

[10] K Hess, H Morkoc, H Shichijo, and B G. Streetman, "Negative differential resistance through real-space electron transfer," *Appl. Phys. Lett.*, vol. 35, no 6, pp. 469–471, Sept. 15, 1979.

[11] Y K Chen, D C. Radulescu, F E. Najjar, and L. F. Eastman, "High frequency instability in a AlGaAs/InGaAs/GaAs double heterojunction MODFET" presented at WOCSEMMAD Workshop, Hilton Head Island, SC, Mar 1987.

[12] K. Lee, M. S Shur, T J. Drummond, and H. Morkoc, "Current–voltage and capacitance–voltage characteristics of modulation-doped field-effect transistors," *IEEE Trans Electron Devices*, vol. ED-30, pp. 207–212, Mar 1983

[13] L H Camnitz, P. J Tasker, P. A. Maki, H. Lee, J Huang, and L. F Eastman, "The role of charge control on drift mobility in AlGaAs/GaAs MODFET's," presented at 10th Biennial IEEE/Cornell Conf. on Adv. Concepts in High Speed Semicond. Devices & Circuits, Ithaca, NY, July 1985.

[14] K Lee, M S Shur, D J Drummond, and H Morkoc, "Parasitic MESFET in (Al,Ga)As/GaAs modulation doped FET's and MODFET FET characteristics," *IEEE Trans. Electron Devices*, vol. ED-31, pp. 29–35, Jan. 1984.